MONURBS: A Parallelized Fast Multipole Multilevel Code for Analyzing Complex Bodies Modeled by NURBS Surfaces

[1]I. González, [2]E. García, [1]F. Saez de Adana, and [1]M. F. Cátedra

[1]Dept. Ciencias de la Computación. Universidad de Alcalá.
28871 Alcalá de Henares (MADRID) SPAIN
Fax: +34 91 885 6646. E-mail: felipe.catedra@uah.es

[2]Dept. Automática. Universidad de Alcalá.
28871 Alcalá de Henares (MADRID). SPAIN

Abstract − This paper presents a Parallelized Multilevel Fast Multipole (MLFMA) Moment Method (MoM) code for analyzing the scattering and radiation from electrically large complex bodies modeled by Non-Uniform Rational B-Spline Surfaces (NURBS). The bodies are represented by NURBS surfaces which are discretized without remeshing the original geometry. The basis and testing functions are defined and conformed to the exact representation of the geometry. This code has been parallelized using Message Passing Interface (MPI) and it has been successfully applied to the study of large bodies including complex and periodic multilayer structures where the real size and shape are very important.

I. INTRODUCTION

In recent years, the application of the MoM technique to the analysis of scattering from large and arbitrary objects has been achieved [1]. The application of the multilevel fast multipole technique to the MoM significantly reduces the computer requirements of memory and CPU-time for analyzing electrically large objects.

In this paper the MLFMA technique [1] is applied to the analysis of complex objects composed of a perfect or real conducting electric and/or dielectric material, modeled by NURBS surfaces [2]. Using these surfaces, any arbitrary object can be represented with very little amount of information without loss of accuracy. In the application presented, the MLFMA technique is applied to quadrangular patches defined over small pieces of NURBS surfaces. These quadrangles totally conform to the real shape of the bodies under analysis. With the proposed method, it is possible to analyze the scattering field of large and complex bodies, including multilayer conformed periodic structures, taking into account their real finite size and shape. Thus, the electromagnetic kernel works with the original Computer Aided Design (CAD) model obtained from the general designing process and no remeshing of the geometry is required. This means that no representation error is added.

The code has been improved for analyzing bodies composed of conductors and dielectric slabs, both modeled using volumetric rooftops. Both conductors and dielectric slabs can be limited by curved surfaces. Also, when the dielectric slabs are electrically thin, the "thin dielectric sheets" (TDS) approximation ([1]) is considered for reducing the CPU time.

To analyze electrically very large objects, a parallel version of the code has been developed. A MPI [3] paradigm has been used because it can be applied in both distributed memory machines and in shared memory ones. The goal is to analyze large objects with processors with relatively small memory and with an affordable execution time.

II. MODEL DISCRETIZATION

Traditionally the geometrical models are defined by planar facets. The geometrical models for MONURBS are defined by NURBS surfaces. NURBS surfaces are parametric surfaces used as a standard format for exchange in CAD that permits the representation of complex objects with very little data. Figure 1 shows a NURBS surface in the real space and its definition in the parametric space.

The geometrical model is discretized using quadrangular patches fully conformed to the exact shape of the body. Every surface is divided into quadrangular patches, thus resulting in a lower number of subdomains in comparison with other discretization techniques. In [4] the discretization is made in the parametric space, but the problem is that an equally spaced step in the parametric space can result in a non-equally spaced step in the real space. Thus, this can produce a higher number of subdomains in NURBS degenerated points that can give ill-conditioned problems. The new approach produces the discretization in the real space, thus resulting in a quadrangular mesh nearly uniform in the shape and size of the patches. Figure 2 shows the difference between the division in the parametric space and the real space. A lot

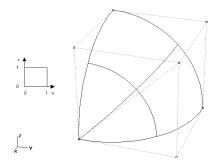of patches are observed near the pole for the division in the parametric space.
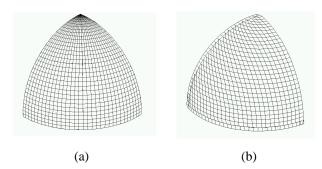

Fig. 1. Example of NURBS surface.

(a)   (b)

Fig. 2. Discretization (a) parametric space and (b) real space.

III. ELECTROMAGNETIC KERNEL

The moment method is applied in the parametric space, so the surface current is defined as,

$$\vec{J}(u,v) = J_u(u,v)\vec{e}_u(u,v) + J_v(u,v)\vec{e}_v(u,v) \qquad (1)$$

where u and v are the parametric coordinates, and $\vec{e}_u(u,v)$ and $\vec{e}_v(u,v)$ vectors are the derivatives in the parametric space.

Modified rooftops and razor-blade functions are used as basis and testing functions, respectively [3]. Both functions conform to the quadrangular meshes previously described that can be arbitrarily curved (see Figs. 3 and 4).
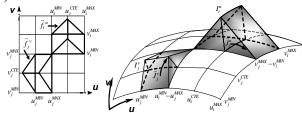

Fig. 3. Basis functions conformed to a curved conducting surface.
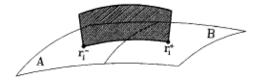

Fig. 4. Testing function conformed to a curve conducting surface.

The electromagnetic kernel of MONURBS can use the Electric Field Integral Equation (EFIE), the Magnetic Field Integral Equation (MFIE), the Combined Field Integral Equation (CFIE) or the Hybrid Integral Equation. For instance, for the EFIE calculation, the coupling between two subdomains i and j is calculated in the parametric space, taking into account both the inductive and the capacitive terms. For the inductive term we have,

$$Z_{ij}^{ind} = \int_{r_i^-}^{r_i^+}\left[\frac{j\omega\mu_0}{4\pi}\int_{S_m}G(\vec{r},\vec{r}')\vec{J}_j^m(\vec{r}')dS'\right]d\vec{l} +$$
$$\int_{r_i^-}^{r_i^+}\left[\frac{j\omega\mu_0}{4\pi}\int_{S_n}G(\vec{r},\vec{r}')\vec{J}_j^n(\vec{r}')dS'\right]d\vec{l} \qquad (2)$$

where $G(\vec{r},\vec{r}')$ is the Green function and m, n are the subpatches that define the subdomain. For the capacitive term,

$$Z_{ij}^{cap} = \int_{r_i^-}^{r_i^+}\left[-\frac{1}{j4\pi\varepsilon_0\omega}\nabla\int_{S_m}\frac{G(\vec{r},\vec{r}')}{S_m}dS'\right]d\vec{l} +$$
$$\int_{r_i^-}^{r_i^+}\left[\frac{1}{j4\pi\varepsilon_0\omega}\nabla\int_{S_n}\frac{G(\vec{r},\vec{r}')}{S_n}dS'\right]d\vec{l} \; . \qquad (3)$$

The calculation of the moment method matrix elements is one of the most computational expensive steps. The integrals shown in equations (3) and (4) are calculated using the Gauss quadrature method. All the surface integrals are evaluated in the rectangular parametric space of the corresponding subpatch (u, v parametric coordinates, shown in Fig. 3). This is not difficult because only a variable change in the integration is required. The computation of the impedance matrix terms is optimized by computing once and storing the value of the integrand functions at the Gaussian integral points. These values are used in many integrals. Also, all the parameters of the subpatches (normalized currents, points, derivatives, etc.) are computed once and stored in the geometrical preprocess to avoid further recomputations when the coupling between subdomains is being calculated.

The Fast Multipole Method (FMM) has been implemented and applied to reduce the memory and CPU-time. The coupling between subdomains is calculated using the multipole approximation [1],

$$Z_{ij} = \frac{jk}{4\pi} \int d^2k \vec{V}_{fmj}(\hat{k}) \cdot \alpha_{mm'}(\hat{k} \cdot \vec{r}_{mm'}) \cdot \vec{V}_{sm'i}^*(\hat{k}) \qquad (4)$$

where $\vec{V}_{sm'i}^*(\hat{k})$, $\alpha_{mm'}(\hat{k} \cdot \vec{r}_{mm'})$ and $\vec{V}_{fmj}(\hat{k})$, respectively are the aggregation, the translation and the disaggregation terms, respectively, of the FMM. The aggregation term is calculated using,

$$\vec{V}_{fmj}(\hat{k}) = \frac{j\omega\mu}{4\pi} \left[\int_{S_m} \vec{J}_j^m(\vec{r}\,') e^{jk\hat{k}\cdot(\vec{r}_c - \vec{r}\,')} dS\,' + \int_{S_n} \vec{J}_j^n(\vec{r}\,') e^{jk\hat{k}\cdot(\vec{r}_c - \vec{r}\,')} dS\,' \right] \quad (5)$$

where m, n are the subpatches of the subdomain, $\hat{k}$ is the wave vector and $\vec{r}_c$ is the center of the FMM region where the subdomain lies. The disaggregation term is calculated using,

$$\vec{V}_{fmi}^*(\hat{k}) = \int_{r_i^-}^{r_i^+} e^{-jk\hat{k}\cdot(\vec{r}_c - \vec{r}\,')} d\vec{l} \cdot \qquad (6)$$

In addition, the MLFMA has been implemented as an extension of the FMM. The number of levels can be chosen by the user. The aggregation and disaggregation terms of the highest levels are obtained from the lowest level terms using interpolation-anterpolation with matrix-vector product [1].

Modified volumetric rooftops and razor-blade functions, [5], defined over curved domains are considered (Fig. 5) for the analysis of dielectric bodies.
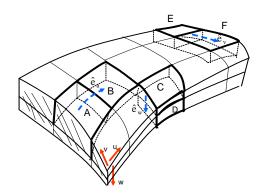

Fig. 5. Basis and testing functions totally conformed to volumetric dielectric bodies.

A parallel version of the code has been developed to be used in both distributed and shared memory machines. This version is based on MPI. The geometry of the problem is immersed into a gridded MLFMA space (Fig. 6). Each processor of the grid computes the coupling that affects the Moment Method unknowns of the cells associated to this processor (computed rigorously or by the multilevel fast multipole approximation). To achieve this goal, each processor needs data computed in others processors. This information is obtained by exchanging explicit messages through a network. All processors

cooperate in the resolution of the system of equations when a problem is solved.
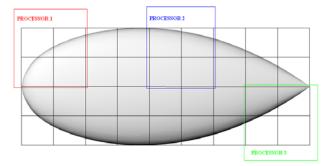

Fig. 6. Problem distribution between processors in the MPI MLFMA application.

IV. RESULTS

Test cases have been tested with MONURBS in several areas of application such as Radar Cross Section, radiation patterns of antennas on board and analysis of multilayer periodic structures like frequency selective surfaces and reflect arrays.

The first case we present here is the analysis of the FLAMME stealth aircraft (see Fig. 7). In this case, a very accurate representation of the actual shape of the aircraft is required. The Bistatic RCS has been obtained for a sweeping angle ϕ ranging from 206º to 360º and $\theta = 90$º at a frequency of 3 GHz.

Fig. 7. Geometrical model of FLAMME aircraft.

Figures 8 and 9 compare the simulated and the measured values for polarizations VV and HH, respectively. A good agreement between the simulations and the measurements can be observed in both figures.

The next example analyzed is the perfect electric conducting NASA almond case shown in Fig. 10. The case was proposed in reference [6]. The geometry is defined by the following parametric equations (all dimensions are in inches),

a) for $-0.416667 < \mathbf{t} < 0$

$$x = dt$$
$$y = 0.193333\,d\left[\sqrt{1-\left(\frac{t}{0.416667}\right)^2}\right]\cos\psi \qquad (6)$$
$$z = 0.06444\,d\left[\sqrt{1-\left(\frac{t}{0.416667}\right)^2}\right]\sin\psi$$
$$-\pi < \psi < \pi$$

b) for $0 < \mathbf{t} < 0.583333$

$$x = dt$$
$$y = 4.833450\,d\left[\sqrt{1-\left(\frac{t}{2.083350}\right)^2}-0.96\right]\cos\psi \qquad (7)$$
$$z = 1.61115d\left[\sqrt{1-\left(\frac{t}{2.083350}\right)^2}-0.96\right]\sin\psi$$
$$-\pi < \psi < \pi$$

where d, the length of the almond, is 9.936 inches. The Monostatic RCS of the almond have been obtained at 7 GHz for HH polarization, $\theta = 90°$ and a sweep angle ϕ ranging from 0° to 180°.

Fig. 8. Measured and computed Bistatic RCS values for FLAMME aircraft, HH polarization.

To show the advantages of the proposed mesh based on NURBS over meshes based on triangular facets, the almond has been analyzed with MONURBS and FIESTA codes. FIESTA is a moment method code that uses a flat triangular mesh, RWG basis functions and a fast direct solution of the moment method linear system of equations, [6]. The almond has been analyzed considering 6, 10, 20, and 40 subdomains per wavelength. The numerical results are also compared between with measurements.

Table 1 shows the number of unknowns required by both numerical approaches for the different number of divisions considered for the geometrical mesh.
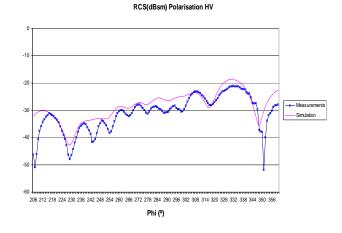

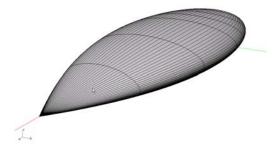Fig. 9. Measured and computed Bistatic RCS values for FLAMME aircraft, HV polarization.

Fig. 10. Geometrical model of the NASA almond.

Table 1. Number of unknowns for the two kinds of meshes considered.

	Unknowns	
Divisions	NURBS	RWG
6	1700	3753
10	4810	8862
20	19730	30492
40	80198	99915

Comparing the results obtained with the NURBS based mesh and the flat faceted mesh, it can be noticed that 6 subdomains per wavelength are not enough to obtain good results. In this case there are several differences between the two numerical approaches and the measurements (Fig. 11). If the number of divisions is increased, the results obtained by the two methods converge to the same values. However, the number of unknowns required by both approaches is different; the mesh based on NURBS requires fewer unknowns than the triangular flat faceted mesh. Comparing with the measurements, both methods provide good results for ten or more subdomains per wavelength (Figs. 12, 13, and 14).
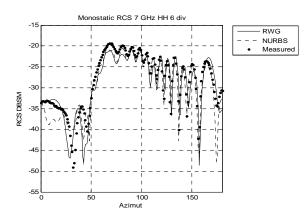
Fig. 11. Comparison between the monostatic numerical RCS values obtained using 6 subdomains per wavelength and measurements.
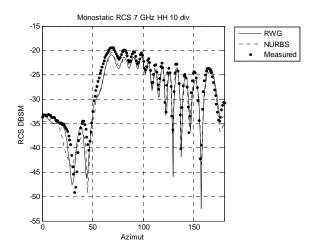
Fig. 12. Comparison between the monostatic numerical RCS values obtained using 10 subdomains per wavelength and measurements.
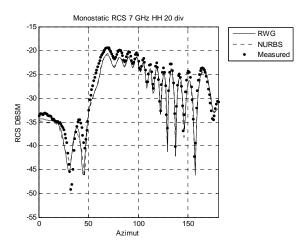
Fig. 13. Comparison between the monostatic numerical RCS values obtained using 20 subdomains per wavelength and measurements.
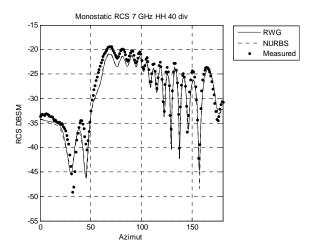
Fig. 14. Comparison between the monostatic numerical RCS values obtained using 40 subdomains per wavelength and measurements.

MONURBS can be also used for obtaining the radiation patterns of antennas on board complex structures. Here the case of an antenna placed on a mock-up of the satellite Jason I is presented. The mock-up has a size of 2.220 m x 1.558 m x 1.507 m and it is shown in Fig. 15 with the antenna location highlighted. This case has been analyzed at 2.2 GHz and the results, shown in Fig. 16 for the cut $\phi = 67.5°$, agree with measurements made by the CNES in an anechoic chamber. The number of unknowns is 152.867 and the simulation lasted for 4 h 28 m on an AMD Opteron 2.4 GHz one processor machine.
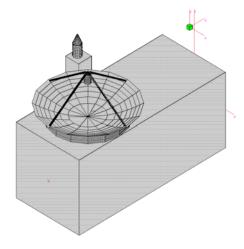
Fig. 15. Geometrical model of Jason-I.

The analysis of multilayer periodic structures could be also conducted with MONURBS using the MLFMA. Several complex multilayer periodic structures have been analyzed and compared with measurements, showing good agreements.
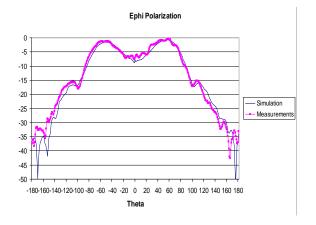
Fig. 16. Comparison between measurements and simulations.

The first complex multilayer periodic structure is the dual three layer reflect array, [7], shown in Fig. 17. The reflect array was designed to generate two pencil beams for TV SAT broadcasting pointing at Europe (11.45 GHz – 12.75 GHz H polarization) and USA (11.45 GHz – 11.7 GHz V-Polarization). The electrical model, shown in Fig. 18, has three layers of periodic structures, several dielectric layers and the ground plane. The reflect array is elliptical with axes at 1036 mm and 980 mm. The number of unknowns considered for the analysis at 12.1 GHz is 1.508.275.
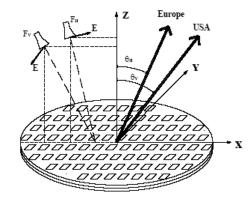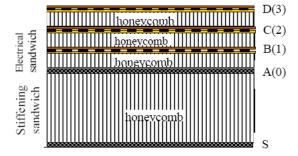

Fig. 17. Three layer reflect array.

Fig. 18. Electrical description of the reflect array.

The results obtained for both polarizations at 12.1 GHz are shown in Figs. 19 and 21, while the measurements are shown in Figs. 20 and 22. For the H polarization, the location of the pencil beam is right, and is so wide like in the measurements. The contour plots of the dBi are at the same level.

For the V polarization, the location of the pencil beam is right and the shape is very similar to this one obtained in the measurements. This polarization is less sensitive to the dielectric effect.
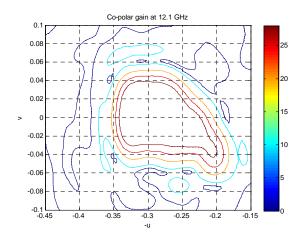

Fig. 19. Contour plot of dBi for the H polarization. Simulation performed at 12.1 GHz.
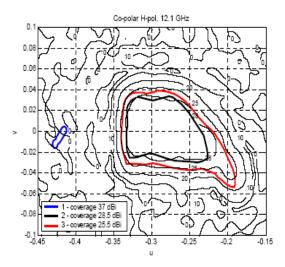

Fig. 20. Contour plot of dBi for the H polarization. Measurements.

The results obtained with the code and the measurements performed at a frequency of 11.05 GHz for the V polarization are shown in Figs. 21 and 22. A good agreement between the simulations and the measurements can be observed.
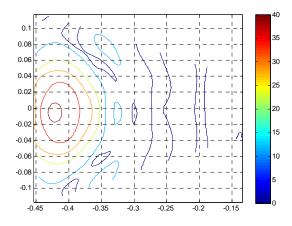
Fig. 21. Contour plot of dBi for V polarization. Simulation performed at 11.05 GHz.

The second periodic structure analyzed is the circular reflect array shown in Fig. 23. It has a radius of 130 mm, a dielectric layer thickness of 0.381 mm and $\varepsilon_r = 2.2$. The primary source is located at (0 mm, 0 mm, 65 mm) and the central design frequency is 94 GHz. This reflect array has been designed and measured by Laboratoire d'Electronique Antennes et Télecommunications, University of Nice, France. Fig. 24 shows the comparisons between the measurements and the simulations for the E plane. There is a good agreement between the measurements and the simulations in a range from 0° to 20°.
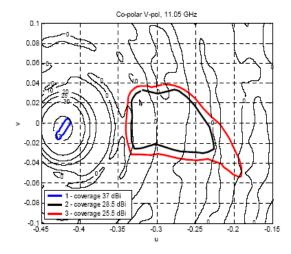

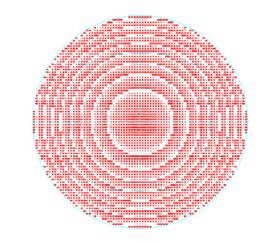Fig. 22. Contour plot of dBi for V polarization. Measurements.
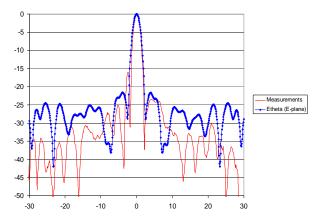

Fig. 23. Circular reflect array.

Fig. 24. Comparison between measurements and simulation for the reflectarray at 94 GHz.

V. CONCLUSIONS

An application of the MLFMA has been presented to the analysis of scattering of complex bodies modeled by NURBS surfaces. These surfaces are a powerful tool to represent complex bodies with accuracy. New basis and testing functions defined over the NURBS surfaces/volumes of the model are considered, reducing the number of unknowns and obtaining good results compared with measurements as is demonstrated through several cases.

A code named MONURBS based on the techniques presented here has been implemented. The code is a versatile tool for successfully analyzing scattering and radiation problems from complex structures. MONURBS is commercially available.

ACKNOWLEDGEMENTS

REFERENCES

[1] W. C. Chew, J. Jin, E. Michielssen, and J. Song, *Fast and efficient algorithms in computational electromagnetics*, Editors. Arctech House INC., 2001.

[2] G. Farin, "Curves and surfaces for computer aided geometric design," Academic Press, 1988.

[3] G. William "Using MPI portable parallel programming with the message-passing interface," The MIT Press, 1999.

[4] L. Valle, F. Rivas, and M. F. Cátedra, "Combining the moment method with geometrical modelling by NURBS surfaces and Bézier patches," *IEEE Transactions on Antennas and Propagation*, vol. 42, no. 3, pp. 373 - 381, March 1994.

[5] S. M. Rao, D. R. Wilton, and A. W. Glisson "Electromagnetic scattering by surfaces of arbitrary shape," *IEEE Transactions on Antennas and Propagation*, pp. 409 - 418, 1982.

[6] A. Heldring, J. M. Rius, J. M. Tamayo, J. Parrón, and E. Ubeda "Fast direct solution of method of moments linear system," *IEEE Transactions on Antennas and Propagation*, vol. 55, no. 11, November 2007.

[7] J. A. Encinar, L. S. Datashvili, J. A. Zornoza, M. Arrebola, M. Sierra-Castaner, J. L. Besada-Sanmartin, H. Baier, and H. Legay, "Dual-polarization dual-coverage reflectarray for space applications," *IEEE Transactions on Antennas and Propagation*, vol. 54, no. 10, pp. 2827 – 2837, October 2006.

Iván González Diego was born in Torrelavega, Spain in 1971. He received the B.S. and M.S. degrees in telecommunications engineering from the University of Cantabria, Spain, in 1994 and 1997 respectively, and the Ph.D degree in telecommunications engineering from the Univeristy of Alcalá , Madrid, Spain in 2004. He worked in the Detectability Laboratory of the National Institute of Technical Aerospace (INTA), Madrid, Spain and as an Assistant Researcher at the University of Alcalá. He currently works as Assistant Professor in this university. He has participated in several research projects with Spanish and European companies, related with analysis of on board antennas, radio propagation in mobile communications, RCS computation, etc. His research interests are in numerical methods applied to the electromagnetic problems, like genetic algorithms and numerical methods to represent complex bodies for the electromagnetic techniques.

Eliseo Garcia was born in Madrid, Spain, in 1977. He received the B.S., M.S. and Ph.D. degrees in telecommunication engineering from the University of Alcalá, Spain, in 1999, 2001 and 2005, respectively. Since 2005, he worked at the University of Alcalá, first as Assistant Professor and since 2006 as Associated Professor in the Automatic Department. His research interests include numerical methods applied to scattering and radiation problems, parallel computing and fast computational techniques applied to electromagnetics.

Francisco Saez de Adana was born in Santander, Spain, in 1972. He received the BS, MS and PhD. degrees in Telecommunications Engineering from the University of Cantabria, Spain, in 1994, 1996 and 2000, respectively. Since 1998 he works at the University of Alcalá, first as assistant professor and since 2002 as professor. He has worked as faculty research at Arizona State University from March 2003 to August 2003. He has participated in more than forty research projects with Spanish, European, American and Japanese companies and universities, related with analysis of on board antennas, radio propagation in mobile communication, RCS computation, etc. He has directed two Ph. D. Dissertations, has published sixteen papers in referred journals and more than 40 conference contributions at international

symposia. His research interests are in areas of high-frequency methods in electromagnetic radiation and scattering, on-board antennas analysis, radio propagation on mobile communications and ray-tracing acceleration techniques.

Manuel F. Catedra received his M.S. and Ph. D. degrees in Telecommunications Engineering from the Polytechnic University of Madrid (UPM) in 1977 and 1982 respectively. From 1976 to 1989 he was with the Radiocommunication and Signal Processing Department of the UPM. He has been Professor at the University of Cantabria from 1989 to 1998. He is currently Professor at the University of Alcalá, in Madrid, Spain.

He has worked on about 60 research projects solving problems of Electromagnetic Compatibility in Radio and Telecommunication Equipment, Antennas, Microwave Components and Radar Cross Section and Mobile Communications. He has developed and applied CAD tools for radio-equipment systems such as Navy-ships, aircraft, helicopters, satellites, the main contractors being Spanish or European Institutions such as EADS, ALCATEL, CNES, ALENIA, ESA, DASA, SAAB, INTA, BAZAN, INDRA, the Spanish Defence Department.

He has directed about 15 Ph D. dissertations, has published about 45 papers (IEEE, Electronic Letters, etc), two books, about 10 chapters in different books, has given short courses and has given around a hundred and thirty presentations in International Symposia.